Theoretical Study of the C(^{3}P) + *trans*-C_4H_8 Reaction

Yan Li, Hui-ling Liu, Xu-ri Huang,* De-Quan Wang, and Chia-chung Sun

State Key Laboratory of Theoretical and Computational Chemistry, Institute of Theoretical Chemistry, Jilin University, Changchun 130023, People's Republic of China

Received: November 24, 2008; Revised Manuscript Received: April 20, 2009

The complex triplet potential energy surface for the reaction of ground-state carbon atom C(^{3}P) with *trans*-C_4H_8 is theoretically investigated at the B3LYP/6-311G(d,p) and G3B3(single-point) levels. Various possible isomerization and dissociation pathways are probed. The initial association between C(^{3}P) and *trans*-C_4H_8 is found to be the C(^{3}P) addition to the C═C bond of *trans*-C_4H_8 to barrierlessly generate the three-membered cyclic isomer **1** $CH_3-cCHCCH-CH_3$. Subsequently, **1** undergoes a ring-opening process to form the chainlike isomer **3a** *cis*−*trans*-$CH_3CHCCHCH_3$, which can either lead to $\mathbf{P_6}(^2CH_3CHCCCH_3 + {}^2H)$ via the C−H bond cleavage or to $\mathbf{P_7}(^2CH_3CHCCH + {}^2CH_3)$ via C−C bond rupture. These two paths are the most favorable channels of the title reaction. Other channels leading to products $\mathbf{P_1}(^2CH_3-cCHCCH + {}^2CH_3)$, $\mathbf{P_2}(^2CH_3-cCHCC-CH_3 + {}^2H)$, $\mathbf{P_3}(trans\text{-}^2CH_3CHCH + {}^2C_2H_3)$, $\mathbf{P_4}(cis\text{-}^2CH_3CHCH + {}^2C_2H_3)$, $\mathbf{P_5}(^3CH_3CH + {}^1CH_3CCH)$, $\mathbf{P_8}(cis\text{-}^2CH_3CHCHCCH_2 + {}^2H)$, $\mathbf{P_9}(trans\text{-}^2CH_3CHCHCCH_2 + {}^2H)$, $\mathbf{P_{10}}(^2CH_3CCCH_2 + {}^2CH_3)$, and $\mathbf{P_{11}}(^2CH_3CHCCHCH_2 + {}^2H)$, however, are much less competitive due to either kinetic or thermodynamic factors. Because the intermediates and transition states involved in the C(^{3}P) + *trans*-C_4H_8 reaction all lie below the reactant, the title reaction is expected to be rapid, as is consistent with the measured large rate constant. Our results may be helpful for future experimental investigation of the title reaction.

1. Introduction

The carbon atom is the fourth most abundant element in universe and especially ubiquitous in dense interstellar clouds (ISCs), where the temperature is very low (10−50 K). It is of great interest due to its involvement in the synthesis and growth of complex hydrocarbons. Particularly, the reactions between the carbon atom in its ground state C(^{3}P) and unsaturated hydrocarbons play important roles in various fields, such as interstellar chemistry,[1,2] hydrocarbon syntheses,[3,4] and combustion processes.[5−7] Up to now, a large number of experimental and theoretical investigations have been reported on the carbon atom C(^{3}P) reactions with a variety of unsaturated hydrocarbons including acetylene (C_2H_2),[8−13] ethylene (C_2H_4),[14] allene (H_2CCCH_2),[15−18] propyne (CH_3CCH),[17−19] propylene (C_3H_6),[18,20] diacetylene (HCCCCH),[21] 1,3-butadiene ($H_2CCHCHCH_2$),[22] and 1,2-butadiene ($H_2CCCHCH_3$)[23] by using crossed-beam techniques or combined ab initio calculations and crossed-beam techniques.

In 2004, Christophe et al. performed experimental studies on the reactions of C(^{3}P) with methylacetylene (CH_3CCH), allene (CH_2CCH_2), propylene (C_3H_6), and *trans*-butene (C_4H_8) at room temperature in a low-pressure fast-flow reactor.[18] Among these reactions, the reaction of C(^{3}P) with *trans*-C_4H_8 attracts our attention. Christophe et al.'s experimental results indicated that the C(^{3}P) + *trans*-C_4H_8 reaction is initiated when the carbon atom attacks the C═C bond of *trans*-C_4H_8, forming an energized adduct; then, the initially formed adduct undergoes further evolution leading to various dissociation products. On the basis of the measured absolute hydrogen branching ratio of 0.33 ± 0.08, Christophe et al. suggested that a H-elimination process is one of the major channels. However, without the information of the potential energy surface of the title reaction, it is difficult to discuss the reaction mechanism. Unfortunately, to our best knowledge, no theoretical studies have been reported on the title reaction up to now. In the present paper, we carried out a detailed theoretical study on the reaction of C(^{3}P) with *trans*-C_4H_8. Our main goals are to (1) provide elaborated isomerization and dissociation channels and (2) investigate the possible products to assist in future experimental studies.

2. Calculation Methods

All of the calculations are carried out using the GAUSSIAN98 and GAUSSIAN03 program packages.[24,25] The optimized geometries and harmonic frequencies of the reactant, products, isomers, and transition states are obtained at the B3LYP/6-311G(d,p) level. Intrinsic reaction coordinate (IRC) calculations are performed at the same level to confirm the connections of transition states between designated isomers. To obtain more reliable energetic data, single-point calculations are performed at the G3B3[26,27] level using the B3LYP/6-311G(d,p)-optimized geometries and scaled B3LYP/6-311G(d,p) zero-point energies.

3. Results and Discussion

Figure 1 depicts the optimized structures of the reactant and products. Figures 2 and 3 depict the optimized structures of isomers and transition states, respectively. The total energy of the reactant C(^{3}P) + *trans*-C_4H_8 is set as zero for reference. The symbol **TSm/n** is used to denote the transition state connecting isomers **m** and **n**. Table 1 lists the total and relative energies of products and various isomers, while those of the transition states are listed in Table 2. The vibrational frequencies (cm^{-1}) and moments of inertia (au) of the reactant, some important products, isomers, and transition states are listed in Table 3. By means of the interrelationship among the reactant, products, isomers, and transition states as well as their relative energies, the schematic potential energy surface (PES) of the C(^{3}P) + *trans*-C_4H_8 reaction at the G3B3//B3LYP/6-311G(d,p) level is presented in Figure 4.

* To whom correspondence should be addressed.

10.1021/jp810312h CCC: $40.75
Published on Web 05/27/2009

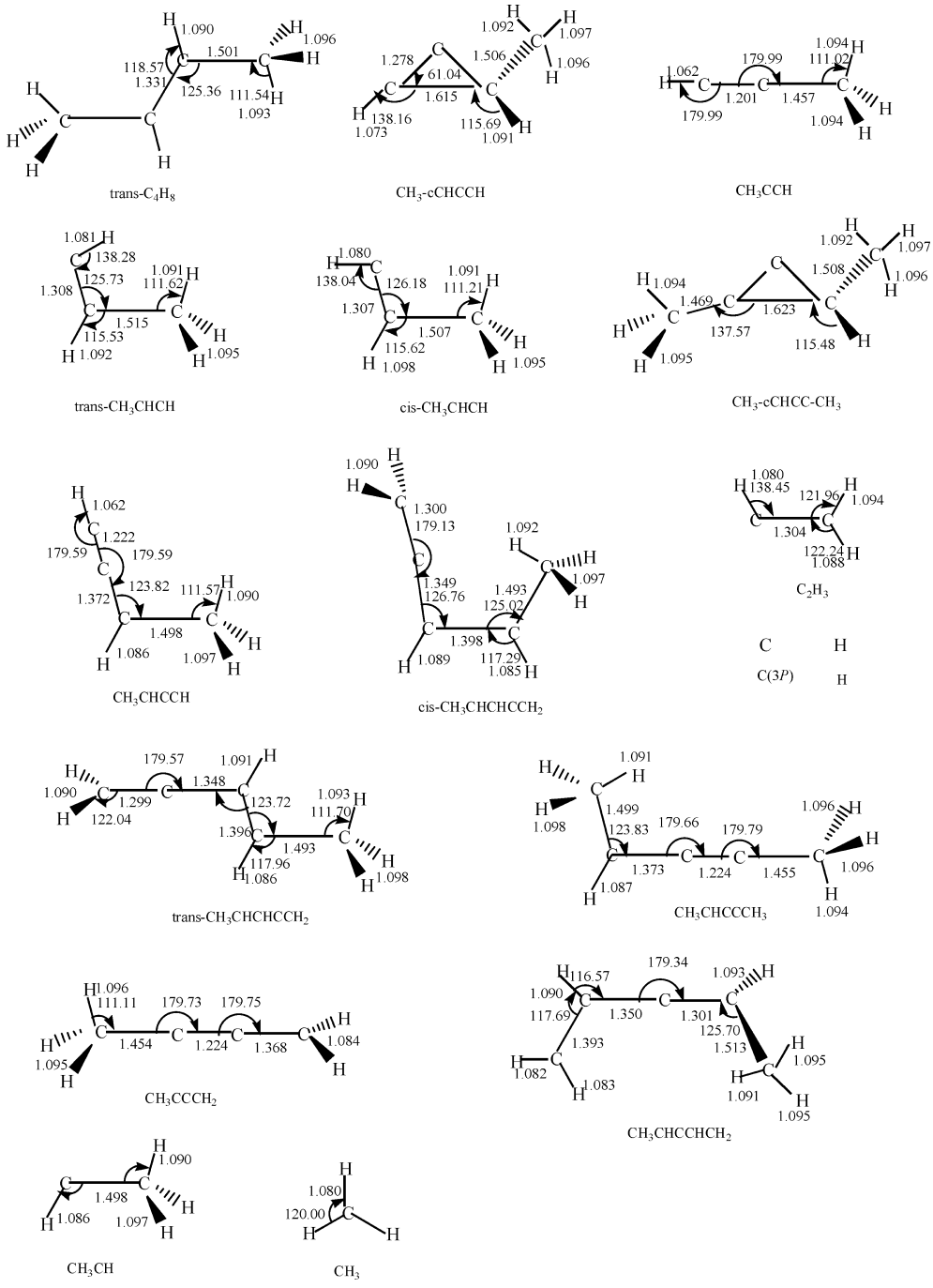

Figure 1. The optimized structures of the reactant and products. Distances are given in angstroms and angles in degrees.

3.1. Entrance Channels. For the C(^{3}P) + *trans*-C_4H_8 reaction, there are two initial attack patterns, that is, (i) the carbon atom C(^{3}P) attacks the C═C bond of *trans*-C_4H_8 to form the three-membered cyclic isomer **1** $CH_3-cCHCCH-CH_3$ (−52.8) and (ii) C(^{3}P) attacks one of the internal C atom of *trans*-C_4H_8 to form the branched-chain-like isomer **14** $CH_3CHCH(C)CH_3$ (−13.0). The values in parentheses are relative energies in kcal/mol with reference to reactant **R** C(^{3}P)+ *trans*-C_4H_8 (0.0). Obviously, formation of the cyclic isomer **1** is thermodynamically favorable. Formation of the branched-chain-like isomer **14** is of little interest. In the following part, we will discuss the formation pathways of various products which associated with isomer **1**.

3.2. Reaction Channels. With the large heat released from the initial step, the three-membered cyclic isomer **1** $CH_3-cCHCCH-CH_3$ can undergo further evolution leading to 11 products, that is, $\mathbf{P_1}$($^2CH_3-cCHCCH$ + $^2CH_3$), $\mathbf{P_2}$-($^2CH_3-cCHCC-CH_3$ + ^2H), $\mathbf{P_3}$(*trans*-$^2CH_3CHCH$ + $^2C_2H_3$), $\mathbf{P_4}$(*cis*-$^2CH_3CHCH$ + $^2C_2H_3$), $\mathbf{P_5}$($^3CH_3CH$ + $^1CH_3CCH$), $\mathbf{P_6}$($^2CH_3CHCCCH_3$ + ^2H), $\mathbf{P_7}$($^2CH_3CHCCH$ + $^2CH_3$), $\mathbf{P_8}$(*cis*-$^2CH_3CHCHCCH_2$ + ^2H), $\mathbf{P_9}$(*trans*-$^2CH_3CHCHCCH_2$ + ^2H), $\mathbf{P_{10}}$($^2CH_3CCCH_2$ + $^2CH_3$), and $\mathbf{P_{11}}$($^2CH_3CHCCCHCH_2$ + ^2H) with the relative energies of −16.5, −11.2, −42.4, −42.9, −38.4, −49.7, −56.7, −48.4 −48.0, −59.5, and −49.4 kcal/mol, respectively.

3.2.1. Formation Pathways of $\mathbf{P_1}$***(*** $^2CH_3-cCHCCH + {}^2CH_3$***) and*** $\mathbf{P_2}$ ***(*** $^2CH_3-cCHCC-CH_3 + {}^2H$***).*** As shown in Figure 4, we find that only one pathway is associated with formation of either $\mathbf{P_1}$ or $\mathbf{P_2}$. They can be written as

Path $\mathbf{P_1}$ R → 1 → $\mathbf{P_1}$

Path $\mathbf{P_2}$ R → 1 → 2 → $\mathbf{P_2}$

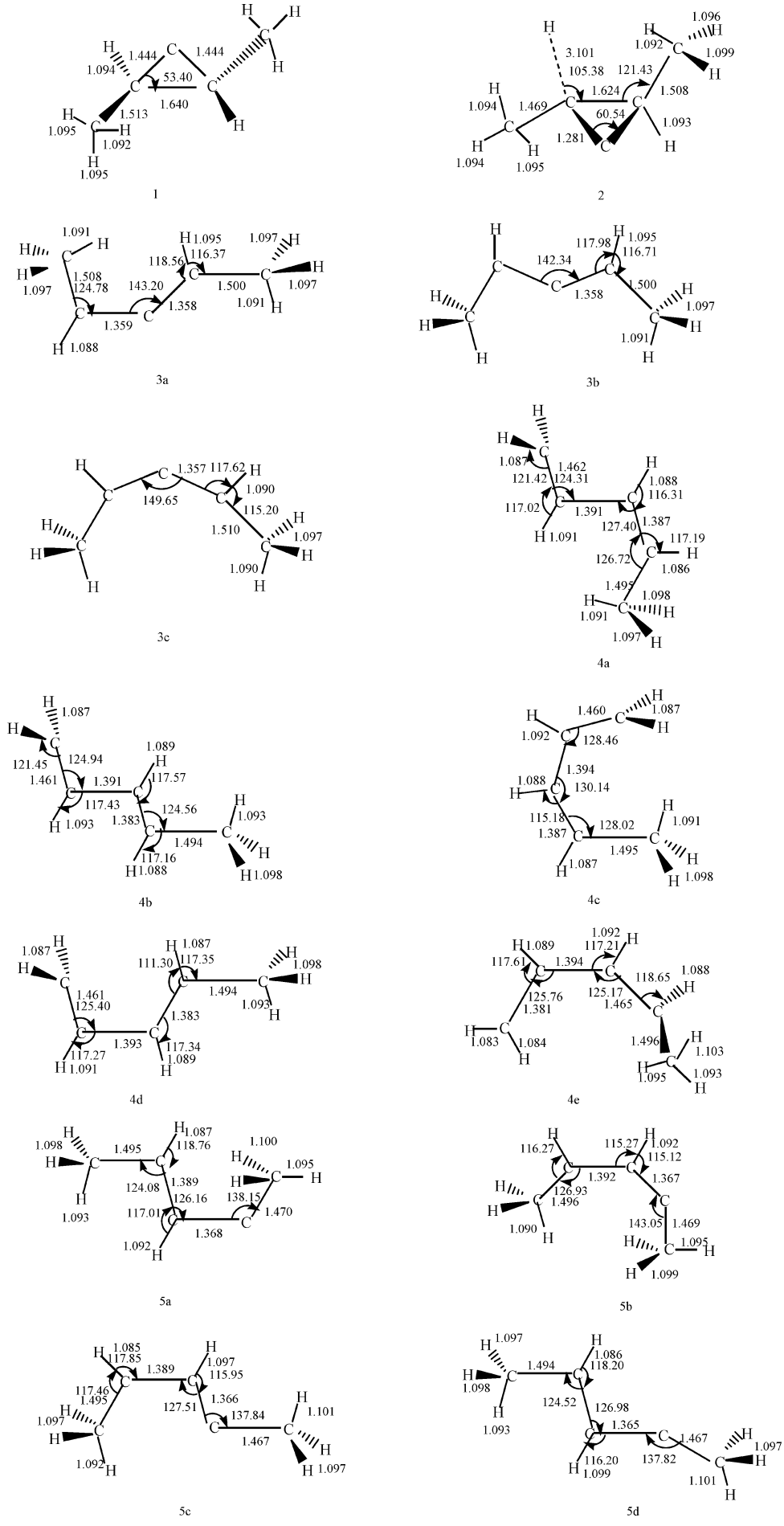

Figure 2. Part 1 of 2. The optimized structures of intermediates. Distances are given in angstroms and angles in degrees.

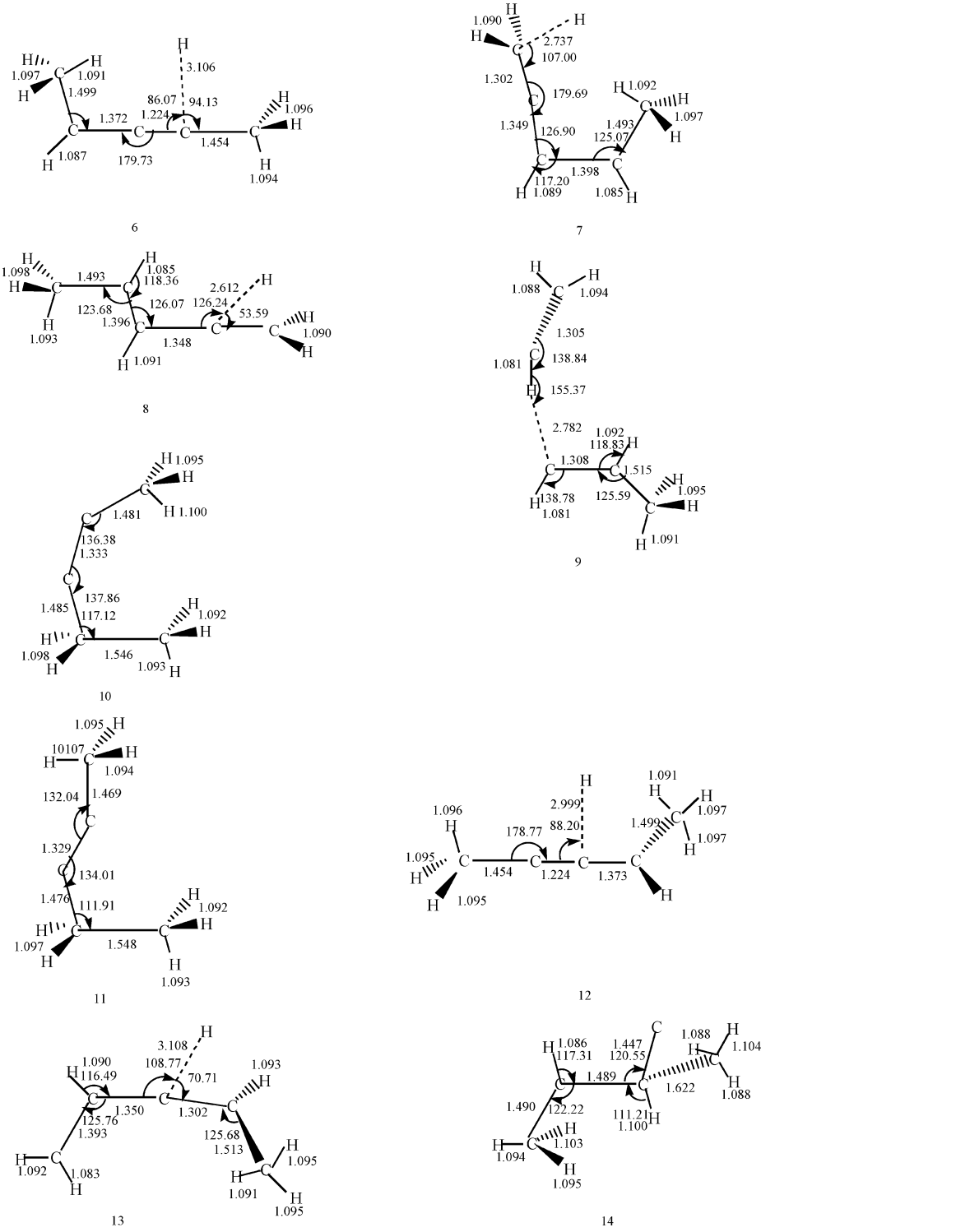

Figure 2. Part 2 of 2.

1 CH_3-cCHCCH$-CH_3$ undergoes CH_3 elimination to form $\mathbf{P_1}$ as in **path** $\mathbf{P_1}$ with the barrier of 42.6 kcal/mol. Alternatively, **1** undergoes H elimination to generate the weakly bound complex **2** CH_3-cCHCC$(CH_3)\cdots$H followed by dissociation to $\mathbf{P_2}$ as in **path** $\mathbf{P_2}$. The conversion barrier of the step **1** → **2** is 45.7 kcal/mol.

3.2.2. Formation Pathway of $\mathbf{P_3}$***(trans-$^2CH_3CHCH$ + $^2C_2H_3$).*** **1** CH_3-cCHCCH$-CH_3$ can transform to the chainlike isomer **3a** *cis*−*trans*-CH_3CHCCHCH_3 via a ring-opening process, followed by isomerization to **3b** *trans*−*trans*-CH_3-CHCCHCH_3. Subsequently, **3b** undergoes a successive 1,3-H shift and C−C bond rupture to form **4b** *trans*−*trans*-CH_3CHCHCHCH_2 and then the weakly bound complex **9** CH_3CHC$H\cdots C_2H_3$. Finally, **9** will dissociate to $\mathbf{P_3}$. The conversion barriers of **1** → **3a**, **3a** → **3b**, **3b** → **4b**, and **4b** → **9** are 12.9, 22.9, 41.1, and 62.8 kcal/mol, respectively. Such multiple processes can be depicted as

Path $\mathbf{P_3}$ **R** → **1** → **3a** → **3b** → **4b** → **9** → $\mathbf{P_3}$

3.2.3. Formation Pathway of $\mathbf{P_4}$***(cis-$^2CH_3CHCH$ + $^2C_2H_3$).*** For product $\mathbf{P_4}$, we find that only one pathway is possible, which can be written as

Path $\mathbf{P_4}$ **R** → **1** → **3a** → **4a** → $\mathbf{P_4}$

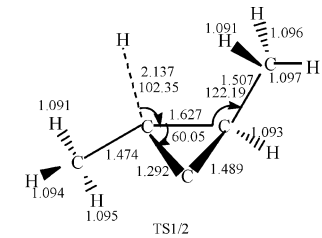

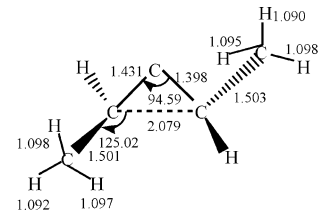

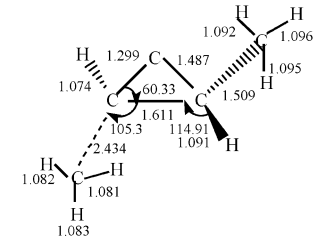

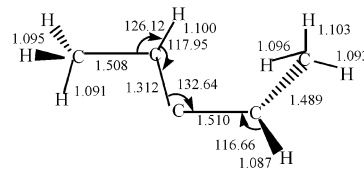

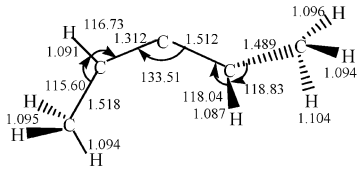

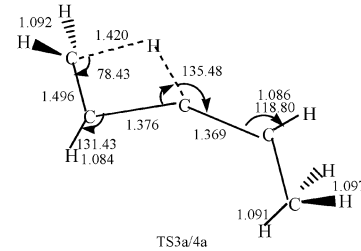

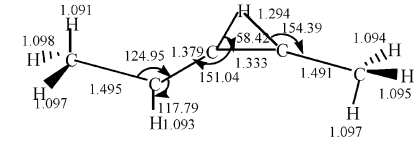

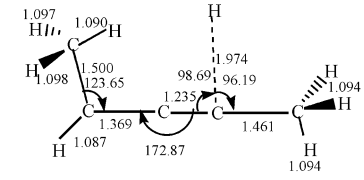

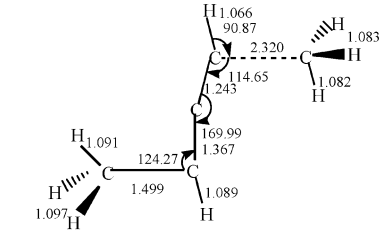

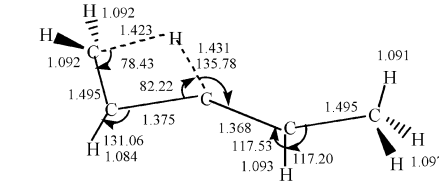

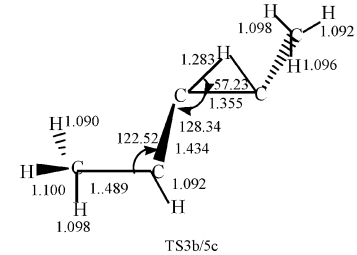

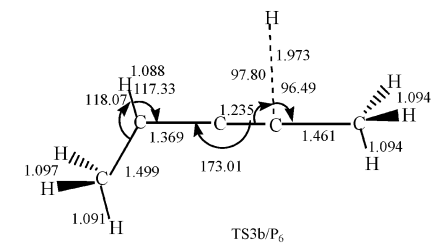

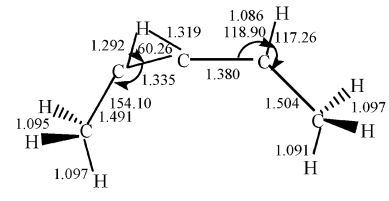

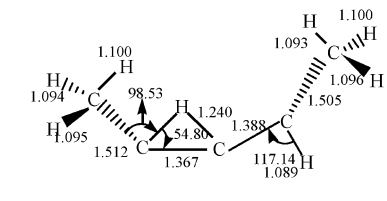

Figure 3. Part 1 of 3. The optimized structures of the transition states. Distances are given in angstroms and angles in degrees.

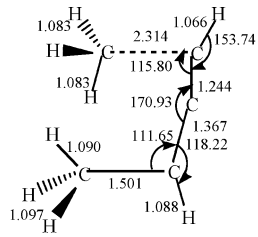

TS3c/P_7

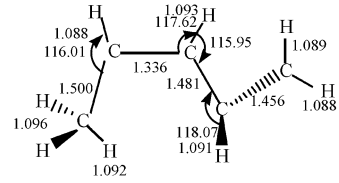

TS4a/4c

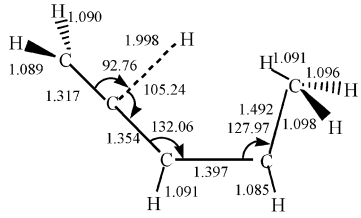

TS4a/7

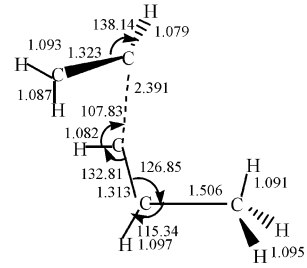

TS4a/P_4

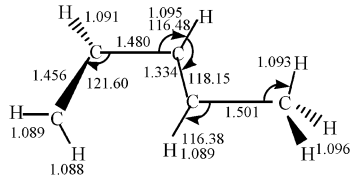

TS4b/4d

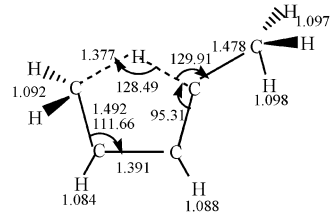

TS4b/5c

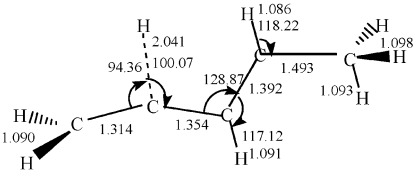

TS4b/8

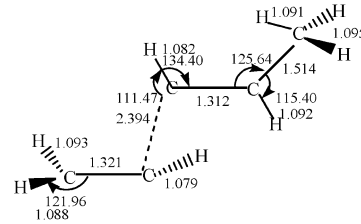

TS4b/9

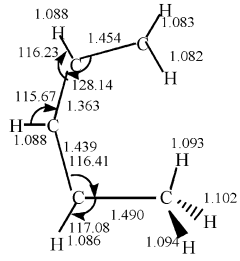

TS4c/4e

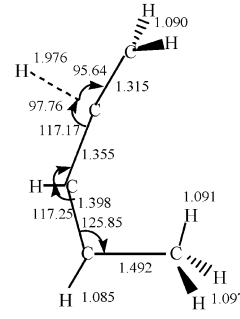

TS4c/P_8

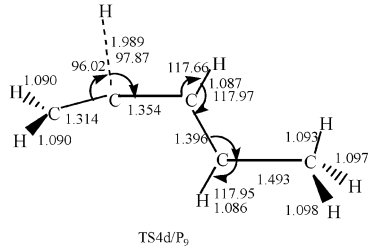

TS4d/P_9

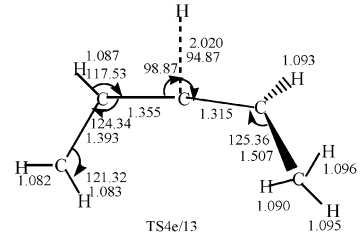

TS4e/13

Figure 3. Part 2 of 3.

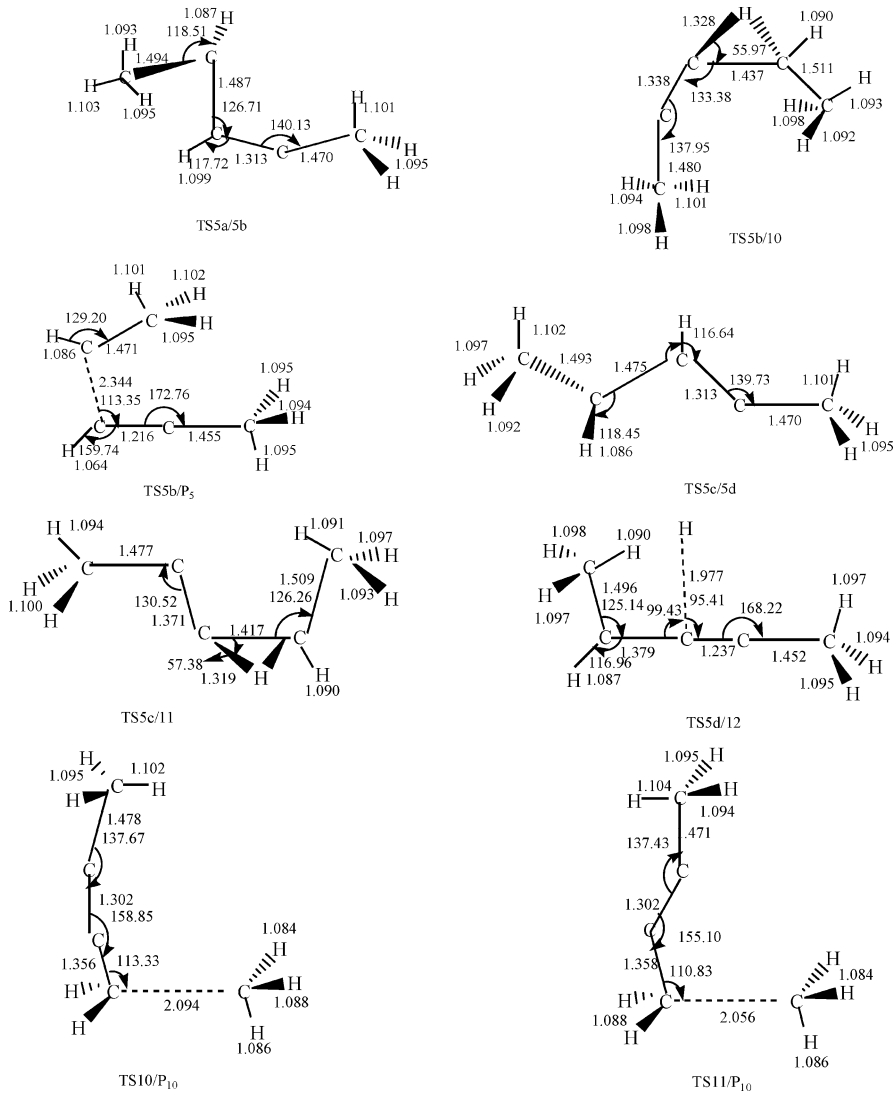

Figure 3. Part 3 of 3.

The formation of **3a** *cis*−*trans*-$CH_3CHCCHCH_3$ is the same as that in path $\mathbf{P_3}$. Subsequently, **3a** undergoes a 1,3-H shift to form **4a** *cis*−*trans*-$CH_3CHCHCHCH_2$ followed by C−C bond fission to yield $\mathbf{P_4}$ with the respective barriers of 41.1 and 62.1 kcal/mol.

3.2.4. Formation Pathway of $\mathbf{P_5}(^3CH_3CH + {}^1CH_3CCH)$**.** There are two feasible pathways to form $\mathbf{P_5}$. They can be written as follows

Path P_5(1) R → 1 → 3a → 5a → 5b → P_5

Path P_5(2) R → 1 → 3a → 3c → 5b → P_5

3a *cis*−*trans*-$CH_3CHCCHCH_3$ can undergo continuously a 2,3-H shift and internal C−C bond rotation to form **5a** *trans*−*cis*-$CH_3CHCHCCH_3$ and then **5b** *cis*−*cis*-$CH_3CHCHCCH_3$ as shown in **path P_5(1)**. In **path P_5(2)**, **3a** undergoes successive internal C−C bond rotation and a 2,3-H shift leading to **3c** *cis*−*cis*-$CH_3CHCCHCH_3$ and then **5b**. Finally, **5b** can dissociate to $\mathbf{P_5}$ via C−C bond rupture.

For **3a → P_5** conversion, three barriers must be surmounted in **path P_5(1)**, which are 47.3, 15.5, and 50.5 kcal/mol for the steps of **3a → 5a**, **5a → 5b**, and **5b → P_5**, respectively, while in **path P_5(2)**, the barriers are 23.5 (**3a → 3c**), 45.9 (**3c → 5b**), and 50.5 (**5b → P_5**) kcal/mol. Thus, we expect that **path P_5(1)** should be competitive with **path P_5(2)**.

3.2.5. Formation Pathway of $\mathbf{P_6}(^2CH_3CHCCCH_3 + {}^2H)$**.** There are five possible pathways for product $\mathbf{P_6}$, as follows

Path P_6(1) R → 1 → 3a → 6 → P_6

Path P_6(2) R → 1 → 3a → 3b → P_6

Path P_6(3) R → 1 → 3a → 3b → 5c → 5d → 12 → P_6

Path P_6(4) R → 1 → 3a → 3b → 4b → 5c → 5d → 12 → P_6

Path P_6(5) R → 1 → 3a → 3c → 5d → 12 → P_6

The formation pathways of **3** (**3a** *cis*−*trans*-$CH_3CHCCHCH_3$, **3b** *trans*−*trans*-$CH_3CHCCHCH_3$, and **3c** *cis*−*cis*-$CH_3CHCCHCH_3$) have been discussed in previous sections. For brevity, we decide not to discuss them again. **3a** can undergo a H-elimination process to form the weakly bound complex **6** $CH_3CHCC(CH_3)\cdots H$ before the final product $\mathbf{P_6}$ as in **path P_6(1)**.

Once **3b** is obtained, several processes may then occur. **3b** can dissociate to $\mathbf{P_6}$ via the C−H bond rupture as in **path P_6(2)**. Alternatively, **3b** can undergo either a 2,3-H shift to form **5c** *cis*−*trans*-$CH_3CHCHCCH_3$ as in **path P_6(3)** or successive a 1,3-H shift and a 1,4-H shift to form **4b** *trans*−*trans*-$CH_3CHCHCHCH_2$ and then **5c**, as in **path P_6(4)**. Subsequently, **5c** can isomerize to **5d** *trans*−*trans*-$CH_3CHCHCCH_3$. On the other hand, a 2,3-H shift of **3c** can also generate **5d** as in **path P_6(5)**. Finally, **5d** undergoes H elimination to form the weakly bound complex **12** $CH_3CHC(\cdots H)CCH_3$ before the final product $\mathbf{P_6}$.

Obviously, **path P_6(1)** and **path P_6(2)** are simpler than the latter three pathways. More importantly, the conversion barriers

TABLE 1: Total (au) and Relative Energies (in parentheses) (kcal/mol) of Reactant, Products, and Isomers at the B3LYP/6-311G(d,p) and G3B3//B3LYP/6-311G(d,p) Levels

species	B3LYP/6-311G(d,p)	G3B3//B3LYP/6-311G(d,p)	
R(C(^{3}P) + *trans*-C_4H_8)	−195.1291496	−194.8936574	(0.0)
P$_1$($^2CH_3$−*c*CHCCH + $^2CH_3$)	−195.1540557	−194.9199089	(−16.5)
P$_2$($^2CH_3$−*c*CHCC−CH_3 + ^2H)	−195.1385081	−194.9114503	(−11.2)
P$_3$(*trans*-$^2CH_3CHCH$ + $^2C_2H_3$)	−195.1828445	−194.9612460	(−42.4)
P$_4$(*cis*-$^2CH_3CHCH$ + $^2C_2H_3$)	−195.1835195	−194.9619975	(−42.9)
P$_5$($^3CH_3CH$ + $^1CH_3CCH$)	−195.1913686	−194.9548108	(−38.4)
P$_6$($^2CH_3CHCCCH_3$ + ^2H)	−195.2045903	−194.9728414	(−49.7)
P$_7$($^2CH_3CHCCH$ + $^2CH_3$)	−195.2210916	−194.9840327	(−56.7)
P$_8$(*cis*-$^2CH_3CHCHCCH_2$ + ^2H)	−195.2029885	−194.9707313	(−48.4)
P$_9$(*trans*-$^2CH_3CHCHCCH_2$ + ^2H)	−195.2028046	−194.9700884	(−48.0)
P$_{10}$($^2CH_3CCCH_2$ + $^2CH_3$)	−195.2268409	−194.9885146	(−59.5)
P$_{11}$($^2CH_3CHCCHCH_2$ + ^2H)	−195.2014152	−194.9723739	(−49.4)
1	−195.2199301	−194.9778730	(−52.8)
2	−195.1385849	−194.9110947	(−10.9)
3a	−195.2731267	−195.0264302	(−83.3)
3b	−195.2742016	−195.0269085	(−83.6)
3c	−195.2703793	−195.0235844	(−81.5)
4a	−195.2798903	−195.0360457	(−89.4)
4b	−195.2815121	−195.0370992	(−90.0)
4c	−195.2783636	−195.0304314	(−85.8)
4d	−195.2816124	−195.0375561	(−90.3)
4e	−195.2820052	−195.0375365	(−90.3)
5a	−195.2753117	−195.0293245	(−85.1)
5b	−195.2729193	−195.0272119	(−83.8)
5c	−195.2765760	−195.0301014	(−85.6)
5d	−195.2763956	−195.0296865	(−85.4)
6	−195.2046653	−194.9725217	(−49.5)
7	−195.2031589	−194.9695168	(−47.6)
8	−195.2031240	−194.9683349	(−46.9)
9	−195.1842113	−194.9467090	(−33.3)
10	−195.2118581	−194.9688483	(−47.2)
11	−195.2056085	−194.9458393	(−32.7)
12	−195.2047517	−194.9726858	(−49.6)
13	−195.2016518	−194.9682649	(−46.8)
14	−195.1578662	−194.9143968	(−13.0)

38.9 (**3** → **6**) kcal/mol in **path P$_6$(1)** and 22.9 (**3a** → **3b**) and 39.2 (**3b** → **P6**) kcal/mol in **path P$_6$(2)** are much lower than the 56.4 (**3b** → **5c**) and 40.6 (**5d** → **12**) kcal/mol in **path P$_6$(4)**, the 41.1 (**3b** → **4b**) and 40.6 (**5d** → **12**) kcal/mol in **path P$_6$(3)**, and the 69.4 (**3c** → **5d**) and 40.6 (**5d** → **12**) kcal/mol in **path P$_6$(5)**. We expect that **path P$_6$(1)** and **path P$_6$(2)** are more competitive than the latter three channels. Furthermore, by comparing the barriers involved in **path P$_6$(1)** and **path P$_6$(2)**, we can deduce that **path P$_6$(1)** is competitive with **path P$_6$(2)**.

***3.2.6. Formation Pathway of* P$_7$(*$^2CH_3CHCCH$ + $^2CH_3$*).** From Figure 4, we find that two pathways are energetically possible to form **P$_7$**, which can be written as

Path P$_7$(1) R → 1 → 3a → P$_7$

Path P$_7$(2) R → 1 → 3a → 3c → P$_7$

3a *cis*−*trans*-$CH_3CHCCHCH_3$ undergoes CH_3 elimination to lead to **P$_7$** with the barrier of 36.3 kcal/mol as in **path P$_7$(1)**, while in **path P$_7$(2)**, **3a** isomerizes to **3c** *cis*−*cis*-$CH_3CHCCHCH_3$ followed by dissociation to **P$_7$** with the respective barriers of 23.5 and 34.6 kcal/mol. Therefore, **path P$_7$(1)** is expected to be the optimal channel to form **P$_7$**.

***3.2.7. Formation Pathway of* P$_8$(*cis-$^2CH_3CHCHCCH_2$ + ^2H*).** For product **P$_8$**, only two pathways are found. They can be written as

Path P$_8$(1) R → 1 → 3a → 4a → 4c → P$_8$

Path P$_8$(2) R → 1 → 3a → 4a → 7 → P$_8$

The formation of **4a** *cis*−*trans*-$CH_3CHCHCHCH_2$ is the same as that in **path P$_4$(1)**. Subsequently, **4a** can either isomerize to **4c** *cis*−*cis*-$CH_3CHCHCHCH_2$ followed by H elimination to generate **P$_8$** as in **path P$_8$(1)** or undergo direct C−H bond cleavage to generate the weakly bound complex **7** $CH_3CHCHCCH_2\cdots H$ before the final product **P$_8$** as in **path P$_8$(2)**.

For **4a** → **P$_8$** conversion, two barriers need to be surmounted in **path P$_8$(1)**, which are 13.4 and 42.9 kcal/mol for the steps of **4a** → **4c** and **4c** → **P$_8$**, respectively. Yet, only one barrier of 49.7 (**4a** → **7**) kcal/mol is present, as in **path P$_8$(2)**. Thus, we expect that **path P$_8$(2)** should be more competitive than **path P$_8$(1)**.

***3.2.8. Formation Pathway of* P$_9$(*trans-$^2CH_3CHCHCCH_2$ + ^2H*).** There are two pathways associated with the formation of **P$_9$**, as follows

Path P$_9$(1) R → 1 → 3a → 3b → 4b → 4d → P$_9$

Path P$_9$(2) R → 1 → 3a → 3b → 4b → 8 → P$_9$

The formation of **4b** *trans*−*trans*-$CH_3CHCHCHCH_2$ is the same as that in **path P$_4$(2)**. **4b** can isomerizes to **4d** *trans*−*cis*-$CH_3CHCHCHCH_2$ followed by H elimination to form **P$_9$** as in **path P$_9$(1)**. The barriers for the steps of **4b** → **4d** and **4d** → **P$_9$** are 13.8 and 47.5 kcal/mol, respectively. In **path P$_9$(2)**, **4b** undergoes H elimination to generate the weakly bound complex **8** $CH_3CHCHC(CH_2)\cdots H$ before the final product **P$_9$**. The barrier for **4b** → **8** conversion is 47.5 kcal/mol. By comparison, we expect that **path P$_9$(2)** should be competitive with **path P$_9$(1)**.

***3.2.9. Formation Pathway of* P$_{10}$(*$^2CH_3CCCH_2$ + $^2CH_3$*).** From Figure 4, we find that four pathways are feasible to form **P$_{10}$**. They can be written as

Path P$_{10}$(1) R → 1 → 3a → 3b → 5c → 11 → P$_{10}$

Path P$_{10}$(2) R → 1 → 3a → 3b → 4b → 5c → 11 → P$_{10}$

Path P$_{10}$(3) R → 1 → 3a → 3c → 5b → 10 → P$_{10}$

TABLE 2: Total (au) and Relative Energies (in parentheses) (kcal/mol) of Transition States at the B3LYP/6-311G(d,p) and G3B3//B3LYP/6-311G(d,p) Levels

species	B3LYP/6-311G(d,p)	G3B3//B3LYP/6-311G(d,p)	
TS1/2	−195.1369734	−194.9050385	(−7.1)
TS1/3a	−195.2010950	−194.9573086	(−39.9)
TS1/P$_1$	−195.1482578	−194.9099391	(−10.2)
TS3a/3b	−195.2319374	−194.9898400	(−60.4)
TS3a/3c	−195.2303412	−194.9888826	(−59.8)
TS3a/4a	−195.2025148	−194.9609772	(−42.2)
TS3a/5a	−195.1928659	−194.9510426	(−36.0)
TS3a/6	−195.2019942	−194.9644845	(−44.4)
TS3a/P$_7$	−195.2101537	−194.9684963	(−47.0)
TS3b/4b	−195.2033102	−194.9613652	(−42.5)
TS3b/5c	−195.1808350	−194.9370230	(−27.2)
TS3b/P$_6$	−195.2020527	−194.9643694	(−44.4)
TS3c/5b	−195.1917463	−194.9504243	(−35.6)
TS3c/5d	−195.1555544	−194.9128947	(−12.1)
TS3c/P$_7$	−195.2096867	−194.9683220	(−46.9)
TS4a/4c	−195.2548011	−195.0147185	(−76.0)
TS4a/7	−195.1941295	−194.9569850	(−39.7)
TS4a/P$_4$	−195.1766524	−194.937172	(−27.3)
TS4b/4d	−195.2552323	−195.0150163	(−76.2)
TS4b/5c	−195.2383828	−194.9961671	(−64.3)
TS4b/8	−195.1983699	−194.9613464	(−42.5)
TS4b/9	−195.1768649	−194.9370796	(−27.2)
TS4c/4e	−195.2720805	−195.0297345	(−85.4)
TS4c/P$_8$	−195.1984227	−194.9620689	(−42.9)
TS4d/P$_9$	−195.1985807	−194.9618991	(−42.8)
TS4e/13	−195.1986133	−194.9620069	(−42.9)
TS5a/5b	−195.2478231	−195.0045763	(−69.6)
TS5b/10	−195.1629182	−194.9199957	(−16.5)
TS5b/P$_5$	−195.1844208	−194.9467755	(−33.3)
TS5c/5d	−195.2482790	−195.0054937	(−70.2)
TS5c/11	−195.1721968	−194.9281893	(−21.7)
TS5d/12	−195.2020010	−194.9650256	(−44.8)
TS10/P$_{10}$	−195.1728488	−194.9297292	(−22.6)
TS11/P$_{10}$	−195.1720892	−194.9299427	(−22.8)

TABLE 3: Vibrational Frequencies and Moments of Inertia of Reactants, Some Important Products, Isomers, and Transition States at the B3LYP/6-311G(d,p) Level of Theory

species	moment of inertia (au)			frequencies (cm^{-1})
trans-C_4H_8	51.6	486.0	515.4	179, 231, 247, 284, 501, 761, 875, 991, 1003, 1068, 1069, 1075, 1166, 1331, 1335, 1415, 1416, 1482, 1482, 1491, 1499, 1742, 3009, 3010, 3050, 3051, 3086, 3088, 3106, 3115
$CH_3CHCCCH_3$	66.3	884.1	928.1	8, 81, 135, 172, 303, 389, 533, 587, 732, 979, 1006, 1032, 1050, 1103, 1235, 1401, 1407, 1421, 1473, 1476, 1477, 1498, 2150, 2993, 3005, 3027, 3053, 3071, 3107, 3140
CH_3CHCCH	46.4	407.9	443.1	85, 211, 381, 436, 552, 597, 646, 867, 1006, 1098, 1151, 1389, 1403, 1476, 1494, 2015, 2998, 3034, 3113, 3148, 3468
CH_3	6.3	6.3	12.6	505, 1403, 1403, 3104, 3283, 3283
1	148.5	541.1	596.3	176, 198, 213, 281, 385, 505, 636, 851, 912,936, 938, 1050, 1076, 1088,1108, 1122,1225, 1330, 1399, 1401, 1409, 1484, 1485, 1491, 1494, 3016, 3017, 3038, 3044, 3071, 3072, 3102, 3103
3a	90.4	803.5	871.6	92, 129, 140, 174, 336, 394, 589, 649, 778, 838, 946, 1013, 1022, 1049, 1110, 1157, 1293, 1384, 1398, 1404, 1459, 1476, 1478, 1494, 1516, 2998, 3001, 3030, 3034, 3041, 3101, 3109, 3123
6	96.6	887.1	961.2	2, 28, 77, 82, 89, 136, 170, 303, 392, 531, 589, 733, 979, 1006, 1031, 1051, 1102, 1234, 1401, 1407, 1421, 1473, 1476, 1477, 1498, 2145, 2994, 3007, 3028, 3054, 3073, 3106, 3140
TS1/3a	105.4	717.5	732.6	i336, 66, 81, 140, 273, 385, 525, 638, 718, 898, 922, 990, 1007, 1043, 1083, 1106, 1209, 1308, 1379, 1393, 1403, 1469, 1475, 1483, 1488, 2993, 3000, 3031, 3052, 3057, 3091, 3111, 3117
TS3a/6	80.2	883.0	940.9	i588, 83, 128, 112, 137, 255, 361, 412, 443, 590, 614, 732, 972, 1006, 1039, 1046, 1099, 1230, 1396, 1404, 1416, 1470, 1477, 1478, 1496, 2066, 2997, 3017, 3035, 3069, 3085, 3113, 3139
TS3a/P$_7$	107.3	959.6	1043.5	i474, 33, 92, 93, 116, 236, 389, 470, 473, 487, 540, 640, 712, 824, 863, 1008, 1086, 1147, 1381, 1402, 1413, 1420, 1476, 1493, 1870, 2997, 3033, 3089, 3105, 3119, 3247, 3256, 3403

Path P$_{10}$(4) R → 1 → 3a → 5a → 5b → 10 → P$_{10}$

The formation pathways of **5b** *cis*−*cis*-$CH_3CHCHCCH_3$ and **5c** *cis*−*trans*-$CH_3CHCHCCH_3$ have been discussed previously. In **path P$_{10}$(1)** and **path P$_{10}$(2)**, **5c** undergoes a 2,3-H shift to form **11** *trans*-$CH_3CH_2CCCH_3$, followed by CH_3 elimintion leading to **P$_{10}$**, while in **path P$_{10}$(3)** and **path P$_{10}$(4)**, **5b**

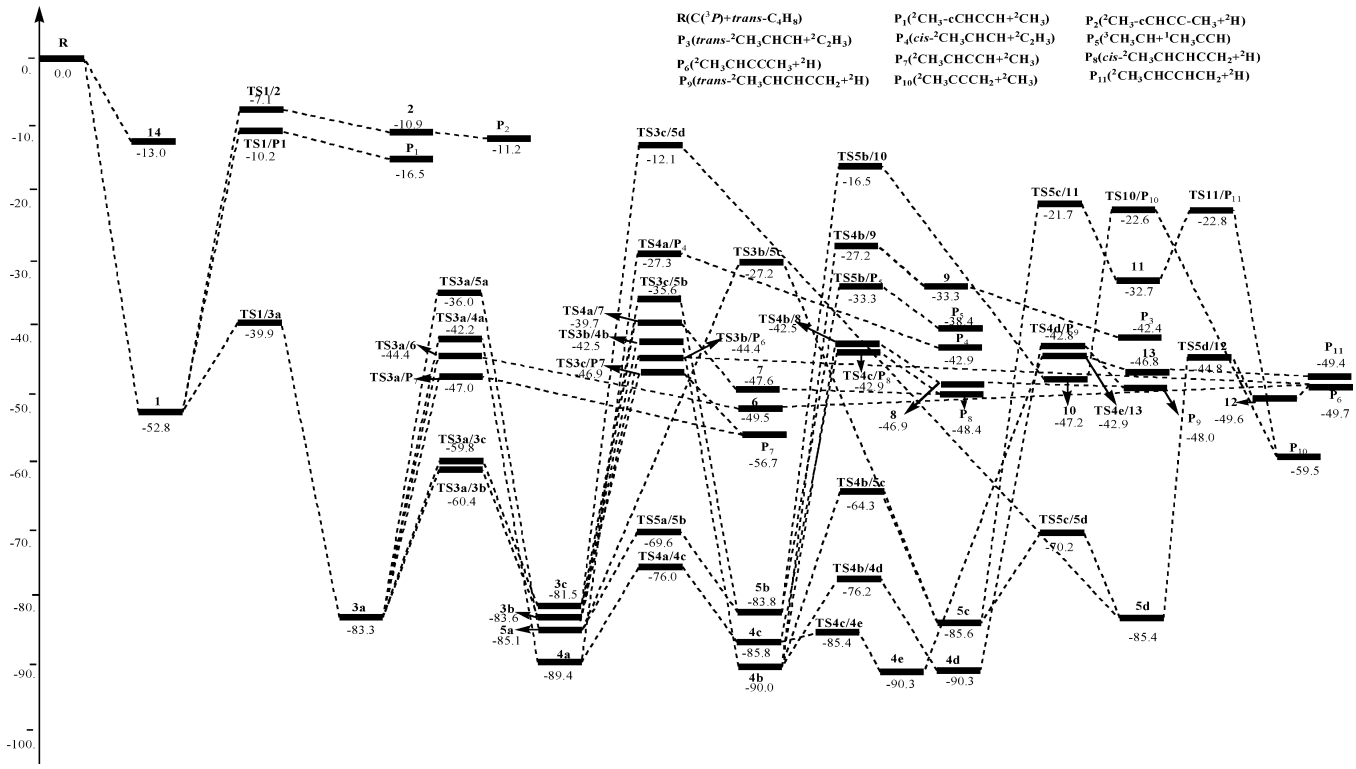

Figure 4. The sketch map of the potential energy surface (PES).

undergoes a 2,3-H shift to generate **10** *cis*-$CH_3CH_2CCCH_3$, and then, **10** will dissociation to $\mathbf{P_{10}}$.

The rate-determining transition state **TS5b/10** (−16.5) in **path $\mathbf{P_{10}}$(3−4)** lies higher than **TS5c/11** (−21.7) in **path $\mathbf{P_{10}}$(1−2)**. Thus, we expect that **path $\mathbf{P_{10}}$(1−2)** may be more competitive than the latter two paths.

Now, let us compare the feasibility of **path $\mathbf{P_{10}}$(1)** and **path $\mathbf{P_{10}}$(2)**. For **3b → 5c** conversion, one high barrier of 56.4 (**3b → 5c**) kcal/mol must be surmounted in **path $\mathbf{P_{10}}$(1)**. While in **path $\mathbf{P_{10}}$(2)**, two moderate barriers have to be surmounted, which are 41.1 and 25.7 kcal/mol for **3b → 4b** and **4b → 5c** conversions, respectively. In addition, the transition state **TS3b/5c** (−27.2) in **path $\mathbf{P_{10}}$(1)** is significantly higher than **TS3b/4b**(−42.5) and **TS4b/5c**(−64.3) in **path $\mathbf{P_{10}}$(2)**. Therefore, **path $\mathbf{P_{10}}$(2)** should be the optimal channel to form $\mathbf{P_{10}}$.

3.2.10. Formation Pathway of $\mathbf{P_{11}}$(^{2}CH$_3$CHCCHCH$_2$ + ^{2}H). The formation of **4c** *cis*−*cis*-$CH_3CHCHCHCH_2$ is the same as that in path **P_9(2)**. **4c** can isomerize to **4e** *cis*-$CH_3CHCHCHCH_2$ with a small barrier of 0.4 kcal/mol. Subsequently, **4e** undergoes a H-elimination process to produce the weakly bound complex **13** $CH_3CHC(C_2H_3)\cdots H$ before the final product $\mathbf{P_{11}}$. The barrier for **4e → 13** conversion is 47.4 kcal/mol. Such a multistep process can be written as:

Path $\mathbf{P_{11}}$ R → 1 → 3a → 4a → 4c → 4e → 13 → $\mathbf{P_{11}}$

4. Reaction Mechanism

In the preceding sections, we have obtained eleven products, that is, $\mathbf{P_1}$(^{2}CH$_3$−*c*CHCCH + ^{2}CH$_3$), $\mathbf{P_2}$(^{2}CH$_3$−*c*CHCC−CH$_3$ + ^{2}H), $\mathbf{P_3}$(*trans*-^{2}CH$_3$CHCH + ^{2}C$_2$H$_3$), $\mathbf{P_4}$(*cis*-^{2}CH$_3$CHCH + ^{2}C$_2$H$_3$), $\mathbf{P_5}$(^{3}CH$_3$CH + ^{1}CH$_3$CCH), $\mathbf{P_6}$(^{2}CH$_3$CHCCCH$_3$ + ^{2}H), $\mathbf{P_7}$(^{2}CH$_3$CHCCH + ^{2}CH$_3$), $\mathbf{P_8}$(*cis*-^{2}CH$_3$CHCHCCH$_2$ + ^{2}H), $\mathbf{P_9}$(*trans*-^{2}CH$_3$CHCHCCH$_2$ + ^{2}H), $\mathbf{P_{10}}$(^{2}CH$_3$CCCH$_2$ + ^{2}CH$_3$), and $\mathbf{P_{11}}$(^{2}CH$_3$CHCCHCH$_2$ + ^{2}H). For convenient discussion, we list the most favorable formation channels for these eleven products again:

Path $\mathbf{P_1}$ R → 1 → $\mathbf{P_1}$
Path $\mathbf{P_2}$ R → 1 → 2 → $\mathbf{P_2}$
Path $\mathbf{P_3}$ R → 1 → 3a → 3b → 4b → 9 → $\mathbf{P_3}$
Path $\mathbf{P_4}$ R → 1 → 3a → 4a → $\mathbf{P_4}$
Path $\mathbf{P_5}$(1) R → 1 → 3a → 5a → 5b → $\mathbf{P_5}$
Path $\mathbf{P_6}$(1) R → 1 → 3a → 6 → $\mathbf{P_6}$
Path $\mathbf{P_7}$(1) R → 1 → 3a → $\mathbf{P_7}$
Path $\mathbf{P_8}$(2) R → 1 → 3a → 4a → 7 → $\mathbf{P_8}$
Path $\mathbf{P_9}$(2) R → 1 → 3a → 3b → 4b → 8 → $\mathbf{P_9}$
Path $\mathbf{P_{10}}$(2) R → 1 → 3a → 3b → 4b → 5c → 11 → $\mathbf{P_{10}}$
Path $\mathbf{P_{11}}$ R → 1 → 3a → 4a → 4c → 4e → 13 → $\mathbf{P_{11}}$

Products $\mathbf{P_1}$ and $\mathbf{P_2}$ lie far above the other nine products; thus, they are unlikely to be detected in the experiment.

Now, let us compare the formation pathways of the remaining nine products. Obviously, **path $\mathbf{P_6}$(1)** and **path $\mathbf{P_7}$(1)** involve simple isomerization and dissociation processes with relatively low barriers, whereas **path$\mathbf{P_3}$−$\mathbf{P_5}$** and **path $\mathbf{P_9}$−$\mathbf{P_{12}}$** proceed via more complicated processes with much higher barriers. For example, the conversion barriers of 41.1 (**3b → 4b**) and 62.8 (**4b → 9**) kcal/mol in **path $\mathbf{P_3}$**, 41.1 (**3a → 4a**) and 62.1 (**4a → $\mathbf{P_4}$**) kcal/mol in **path $\mathbf{P_4}$**, 47.3 (**3a → 5a**) and 50.5 (**5b → $\mathbf{P_5}$**) in **path $\mathbf{P_5}$**, 41.1 (**3a → 4a**) and 49.7 (**4a → 7**) kcal/mol in **path $\mathbf{P_8}$**, 41.1 (**3b → 4b**) and 47.5 (**4b → 8**) in **path $\mathbf{P_9}$**, 41.1 (**3b → 4b**) and 63.9 (**5c → 11**) kcal/mol in **path $\mathbf{P_{10}}$**, and 41.1 (**3a → 4a**) and 47.4 (**4e → 13**) kcal/mol in **path $\mathbf{P_{11}}$** are considerablely larger than those in **path $\mathbf{P_6}$(1)** and **path $\mathbf{P_7}$(1)**, that is, 38.9 (**3a → 6**) kcal/mol in **path $\mathbf{P_6}$** and 36.3 (**3a → $\mathbf{P_7}$**) kcal/mol in **path $\mathbf{P_7}$**. Therefore, **path $\mathbf{P_6}$(1)** and **path $\mathbf{P_7}$(1)** should be the most feasible channels; other channels are energetically inaccessible due to the high barriers, and thus, they are of negligible importance. Because the barriers involved in **path $\mathbf{P_6}$(1)** and **path $\mathbf{P_7}$(1)** are very close, these two channels may compete with each other. As a result, reflected in the final product distributions, $\mathbf{P_6}$ and $\mathbf{P_7}$ should be the most feasible products with comparative

yields; other products may have undetected yields due to either kinetic or thermodynamic factors.

5. Comparison with Experiments

It is worthwhile to make comparison between our calculated results and previous experimental findings for the $C(^3P) + trans\text{-}C_4H_8$ reaction. The measured room temperature rate constant is $k = (1.9 \pm 0.6) \times 10^{10}$cm^3 molecule^{-1} s^{-1}, indicating that this reaction is very fast. This point can be explained by the overall barrierless association, isomerization, and dissociation processes of the title reaction. On the basis of the measured absolute hydrogen branching ratio (0.33 ± 0.08), Christophe et al. suggested that H abstraction is one of the major channels. This is in good agreement with our theoretical results that $\mathbf{P_6}(^2CH_3CHCCCH_3 + {}^2H)$ is one of the major products. On the other hand, according to our calculations, the CH_3-elimiantion product $\mathbf{P_7}(^2CH_3CHCCH + {}^2CH_3)$ is also a major product of the title reaction, which means that the $C(^3P) + trans\text{-}C_4H_8$ reaction cannot play an important role in synthesizing a long carbon chain in the interstellar medium. Our calculation results may be helpful to further theoretical and experimental investigation of the $C(^3P) + trans\text{-}C_4H_8$ reaction.

6. Interstellar Implications

It is generally known that reactions with zero or minute barriers are favorable to take place in the interstellar medium (ISM) where the temperature is very low. The barrierless nature of the total reaction makes the $C(^3P) + trans\text{-}C_4H_8$ reaction proceed very easy and leads to the major products $\mathbf{P_6}(^2CH_3CHCCCH_3 + {}^2H)$ and $\mathbf{P_7}(^2CH_3CHCCH + {}^2CH_3)$. The CH_3 radical is an important intermediate in the interstellar medium driven by cosmic-ray ionization[28] as well as in the combustion process.[29] The CH_3CHCCH radical is a promising species because it possesses the possible importance in the ring-formation processes; however, these processes require further investigations. Fortunately, Miller and Melius[30] suggested that the isomerization between CH_3CHCCH and $CH_2CHCHCH$ plays a crucial role in the formation of benzene during the process of C_2H_2 reactions with CH_3CHCCH. This indicates that the CH_3CHCCH radical maybe play an important role in the ring-formation processes. Up to now, there has been a number of experimental and theoretical studies reported on the CH_3CHCCH radical.[31−38] In contrast, the $CH_3CHCCCH_3$ radical has received rather little attention, and our calculated results may provide an insight into the formation mechanism of $CH_3CHCCCH_3$. Furthermore, the H atom is important in the H-containing system. All of the aspects mentioned above reinforce the importance of the $C(^3P) + trans\text{-}C_4H_8$ reaction in the interstellar medium.

7. Conclusion

A detailed theoretical study was performed on the $C(^3P) + trans\text{-}C_4H_8$ reaction. Our calculation results show that the ground-state carbon atom $C(^3P)$ can barrierlessly attack the C=C bond of $trans\text{-}C_4H_8$ to form the three-membered cyclic isomer **1** $CH_3-cCHCCH-CH_3$, followed by further evolution leading to 11 products. Among these products, $\mathbf{P_6}(^2CH_3CHCCCH_3 + {}^2H)$ and $\mathbf{P_7}(^2CH_3CHCCH + {}^2CH_3)$ are the major products with comparable abundance, while the other products may have undetected yields. Our calculation results are in good agreement with the experimental studies of the $C(^3P) + trans\text{-}C_4H_8$ reaction, and we hope that our results may provide useful information for understanding the effect of the carbon atom $C(^3P)$ toward other unsaturated hydrocarbons.

Acknowledgment. This work was supported by the National Natural Science Foundation of China (No20773048).

References and Notes

(1) Clary, D. C.; Buonomo, E.; Sims, I. R.; Smith, I. W. M.; Geppert, W. D.; Naulin, C.; Costes, M.; Cartechini, L.; Casavecchia, P. *J. Phys. Chem. A* **2002**, *106*, 5541.
(2) Smith, I. W. M. *Chem. Soc. Rev.* **2003**, *31*, 137.
(3) Clary, D. C.; Haider, N.; Husain, D.; Kabir, M. *Astrophys. J.* **1994**, *422*, 416.
(4) Turner, B. E.; Herbst, E.; Terzieva, R. *Astrophys. J., Suppl. Ser.* **2000**, *126*, 427.
(5) Kaiser, R. I.; Le, T. N.; Nguyen, T. L.; Mebel, A. M.; Balucani, N.; Lee, Y. T.; Stahl, F.; Schleyer, P. v. R.; Schaefer, H. F., III *Faraday Discuss.* **2001**, *119*, 51.
(6) Casavecchia, P.; Balucani, N.; Cartechini, L.; Capozza, G.; Bergeat, A.; Volpi, G. G. *Faraday Discuss.* **2001**, *119*, 27.
(7) Kaiser, R. I.; Mebel, A. M. *Int. Rev. Phys. Chem* **2002**, *21*, 307.
(8) Haider, N.; Husain, D. J. *Chem. Soc., Faraday Trans.* **1993**, *89*, 7.
(9) Clary, D. C.; Haider, N.; Husain, D.; Kabir, M. *Astrophys. J.* **1994**, *422*, 416.
(10) Kaiser, R. I.; Lee, Y. T.; Suits, A. G. *J. Chem. Phys.* **1995**, *103*, 10395.
(11) Takayanagi, T. *J. Phys. Chem. A* **2006**, *110*, 361.
(12) Mebel, A. M.; Kislov, V. V.; Hayasi, M. *J. Chem. Phys.* **2007**, *126*, 204310.
(13) Leonori, F.; Petrucci, R.; Segoloni, E.; Bergeat, A.; Hickson, K. M.; Balucani, N.; Casavecchia, P. *J. Phys. Chem. A* **2008**, *112*, 1363.
(14) Kaiser, R. I.; Lee, Y. T.; Suits, A. G. *J. Chem. Phys.* **1996**, *105*, 8705.
(15) Kaiser, R. I.; Mebel, A. M.; Chang, A. H. H.; Lin, S. H.; Lee, Y. T. *J. Chem. Phys.* **1999**, *110*, 10330.
(16) Schranz, H. W.; Smith, S. C.; Mebel, A. M.; Lin, S. H. *J. Chem. Phys.* **2002**, *117*, 7055.
(17) Mebel, A. M.; Kaiser, R. I.; Lee, Y. T. *J. Am. Chem. Soc.* **2000**, *122*, 1776.
(18) Loison, J. C.; Bergeat, A. *Phys. Chem. Chem. Phys.* **2004**, *6*, 5396.
(19) Kaiser, R. I.; Stranges, D.; Lee, Y. T.; Suits, A. G. *J. Chem. Phys.* **1996**, *105*, 8721.
(20) Kaiser, R. I.; Stranges, D.; Bevsek, H. M.; Lee, Y. T.; Suits, A. G. *J. Chem. Phys.* **1997**, *106*, 4945.
(21) Sun, B. J.; Huang, C. Y.; Kuo, H. H.; Chen, K. T.; Sun, H. L.; Huang, C. H.; Tsai, M. F.; Kao, C. H.; Wang, Y. S.; Gao, L. G.; Kaiser, R. I.; Chang, A. H. H. *J. Chem. Phys.* **2008**, *128*, 244303.
(22) Hahndorf, I.; Lee, H. Y.; Mebel, A. M.; Lin, S. H.; Lee, Y. T.; Kaiser, R. I. *J. Chem. Phys.* **2000**, *113*, 9622.
(23) Balucani, N.; Lee, H. Y.; Mebel, A. M.; Kaiser, R. I. *J. Chem. Phys.* **2001**, *115*, 5107.
(24) Frisch, M. J.; Trucks, G. W.; Schlegel, H. B.; Scusera, G. E.; Robb, M. A.; Cheeseman, J. R.; Zakrzewski, V. G.; Montgomery, J. A.; Stratmann, R. E., Jr.; Burant, J. C.; Dapprich, S.; Millam, J. M.; Daniels, A. D.; Kudin, K. N.; Strain, M. C.; Farkas, O.; Tomasi, J.; Barone, V.; Cossi, M.; Cammi, R.; Mennucci, B.; Pomelli, C.; Adamo, C.; Clifford, S.; Ochterski, J.; Petersson, G. A.; Ayala, P. Y.; Cui, Q.; Morokuma, K.; Malick, D. K.; Rabuck, A. D.; Raghavachari, K.; Foresman, J. B.; Cioslowski, J.; Ortiz, J. V.; Baboul, A. G.; Stefanov, B. B.; Liu, G.; Liashenko, A.; Piskorz, P.; Komaromi, I.; Gomperts, R.; Martin, R. L.; Fox, D. J.; Keith, T.; Al-Laham, M. A.; Peng, C. Y.; Nanayakkara, A.; Gonzalez, C.; Challacombe, M.; Gill, P. M. W.; Johnson, B.; Chen, W.; Wong, M. W.; Andres, J. L.; Gonzalez, C.; Head-Gordon, M.; Replogle, E. S.; Pople, J. A. *Gaussian 98*, revision A.6; Gaussian, Inc.: Pittsburgh, PA, 1998.
(25) Frisch, M. J.; Trucks, G. W.; Schlegel, H. B.; Scuseria, G. E.; Robb, M. A.; Cheeseman, J. R.; Montgomery, J. A., Jr.; Vreven, T.; Kudin, K. N.; Burant, J. C.; Millam, J. M.; Iyengar, S. S.; Tomasi, J.; Barone, V.; Mennucci, B.; Cossi, M.; Scalmani, G.; Rega, N.; Petersson, G. A.; Nakatsuji, H.; Hada, M.; Ehara, M.; Toyota, K.; Fukuda, R.; Hasegawa, J.; Ishida, M.; Nakajima, T.; Honda, Y.; Kitao, O.; Nakai, H.; Klene, M.; Li, X.; Knox, J. E.; Hratchian, H. P.; Cross, J. B.; Bakken, V.; Adamo, C.; Jaramillo, J.; Gomperts, R.; Stratmann, R. E.; Yazyev, O.; Austin, A. J.; Cammi, R.; Pomelli, C.; Ochterski, J. W.; Ayala, P. Y.; Morokuma, K.; Voth, G. A.; Salvador, P.; Dannenberg, J. J.; Zakrzewski, V. G.; Dapprich, S.; Daniels, A. D.; Strain, M. C.; Farkas, O.; Malick, D. K.; Rabuck, A. D.; Raghavachari, K.; Foresman, J. B.; Ortiz, J. V.; Cui, Q.; Baboul, A. G.; Clifford, S.; Cioslowski, J.; Stefanov, B. B.; Liu, G.; Liashenko, A.; Piskorz, P.; Komaromi, I.; Martin, R. L.; Fox, D. J.; Keith, T.; Al-Laham, M. A.; Peng, C. Y.; Nanayakkara, A.; Challacombe, M.; Gill, P. M. W.; Johnson, B.; Chen, W.; Wong, M. W.; Gonzalez, C.; Pople, J. A. *Gaussian 03*, revision B.03; Gaussian, Inc.: Wallingford, CT, 2004.

(26) Curtiss, L. A.; Raghavachari, K.; Redfern, P. C.; Rassolov, V.; Pople, J. A. *J. Chem. Phys.* **1998**, *109*, 7764.

(27) Boboul, A. G.; Curtiss, L. A.; Redfern, P. C.; Raghavachari, K. *J. Chem. Phys.* **1999**, *110*, 7650.

(28) Herbst, E.; Klemperer, W. *Appl. Phys. Lett.* **1973**, *185*, 505.

(29) Hughes, K. J.; Turanyi, T.; Clague, A. R.; Pilling, M. J. *Int. J. Chem. Kinet.* **2001**, *33*, 513.

(30) Miller, J. A.; Melius, C. F. *Combust. Flame* **1992**, *91*, 21.

(31) Marinov, N. M.; Pitz, W. J.; Westbrook, C. K.; Lutz, A. E.; Vincitore, A. M.; Senkan, S. M. In *27th Symposium (International) on Combustion Institute*; 1998; pp 605−613.

(32) Parker, C. L.; Cooksy, A. L. *J. Phys. Chem. A* **1999**, *103*, 2160.

(33) Hansen, N.; Klippenstein, S. J.; Taatjes, C. A.; Miller, J. A.; Wang, J.; Cool, T. A.; Yang, B.; Yang, R.; Wei, L.; Huang, C.; Wang, J.; Qi, F.; Law, M. E.; Westmorelane, P. R. *J. Phys. Chem. A* **2006**, *110*, 3670.

(34) Marinov, N. M.; Pitz, W. J.; Westbrook, C. K.; Castaldi, M. J.; Senkan, S. M. *Combust. Soc. Technol.* **1996**, *117*, 211.

(35) Hansen, N.; Cool, T. A.; Westnoreland, P. R.; Kohse-Hõinghaus, K. *Prog. Energy Combust. Sci.* **2009**, *35*, 168.

(36) Nguyen, T. T.; King, K. D. *J. Phys. Chem.* **1981**, *85*, 3130.

(37) Hansen, N.; Miller, J. A.; Taatjes, C. A.; Wang, J.; Cool, T. A.; Law, M. E.; Westmoreland, P. R. *Proc. Combust. Inst.* **2007**, *31*, 1157.

(38) Yang, B.; Li, Y.; Wei, L.; Huang, C.; Wang, J.; Tian, Z.; Yang, R.; Sheng, L.; Zhang, Y.; Qi, F. *Proc. Combust. Inst.* **2007**, *31*, 555.

JP810312H